

Origin of complex exchange anisotropy in Fe/MnF₂ bilayers

I. N. Krivorotov,¹ C. Leighton,² J. Nogués,³ Ivan K. Schuller,⁴ and E. Dan Dahlberg¹

¹*Department of Physics, University of Minnesota, 116 Church Street SE, Minneapolis, Minnesota 55455, USA*

²*Department of Chemical Engineering and Materials Science, University of Minnesota, 421 Washington Avenue SE, Minneapolis, Minnesota 55455, USA*

³*Institució Catalana de Recerca i Estudis Avançats (ICREA) and Departament de Física, Universitat Autònoma de Barcelona, 08193 Bellaterra, Spain*

⁴*Department of Physics, University of California-San Diego, La Jolla, California 92093-0319, USA*

(Received 26 June 2003; published 28 August 2003)

An analytical model of exchange anisotropy in epitaxial ferromagnetic/antiferromagnetic bilayers was developed. The model demonstrates that the high symmetry exchange anisotropy terms in ferromagnetic/antiferromagnetic bilayers originate from a partial domain wall in the antiferromagnetic layer. Application of the model to the experimental data analysis enables one to separately determine the fraction of uncompensated interfacial spins in the antiferromagnetic layer and the interfacial exchange coupling energy between spins in the ferromagnet and in the antiferromagnet. The model provides a quantitative description of complex exchange anisotropy recently observed in Fe/MnF₂ bilayers.

DOI: 10.1103/PhysRevB.68.054430

PACS number(s): 75.70.Cn, 73.50.Jt

Exchange coupling between ferromagnetic (*F*) and anti-ferromagnetic (AF) materials¹ is an outstanding problem in magnetism.² Below the Néel temperature (T_N) of the AF materials this coupling results in dramatic changes of the magnetic properties of the ferromagnet which include a hysteresis loop shift, an enhanced coercivity, and an asymmetry of the magnetization reversal for the increasing and decreasing magnetic fields.^{3–5} Since the energy of the AF/*F* system depends on the direction of the *F* magnetization, \mathbf{M}_F , the AF/*F* exchange coupling results in a magnetic anisotropy called the exchange anisotropy (EA). Although some phenomena originating from the AF/*F* coupling are qualitatively understood, a quantitative microscopic theory of the AF/*F* coupling is lacking.⁶

In this paper we develop an analytical model describing the angular dependence of the EA energy of AF/*F* bilayers with an epitaxial AF layer. The model explains the origin of the high symmetry EA terms recently observed in epitaxial AF/*F* bilayers.^{7–9} These high symmetry terms play important roles in determining the magnetic properties of the AF/*F* bilayers. In particular, the threefold EA term results in an asymmetric magnetization reversal⁷ while the fourfold EA term gives rise to an enhanced coercivity of the bilayers.^{7–9} Application of the model to the experimental data analysis allows one to separately determine the fraction of uncompensated interfacial spins in the AF layer, δ , and the exchange coupling energy J_{in} between an interfacial AF spin and \mathbf{M}_F . This is demonstrated on an example of Fe/MnF₂ bilayers with an epitaxial MnF₂ layer. The model provides a good quantitative description of a surprisingly complex angular dependence of the EA recently found in this system.^{7,8}

MnF₂ is a uniaxial AF material with Mn²⁺ ions ($S = \frac{5}{2}$) forming a body centered tetragonal lattice. The AF easy axis is along the crystallographic *c* axis (lattice constants $a = 4.87 \text{ \AA}$, $c = 3.30 \text{ \AA}$), $T_N = 67 \text{ K}$, and the magnetocrystalline anisotropy $K_{AF} = 4.6 \times 10^6 \text{ erg/cm}^3$.¹⁰ Growth of the Fe/MnF₂ bilayers by *e*-beam evaporation on MgO(100) sub-

strates results in a twinned epitaxial AF layer and a polycrystalline Fe layer¹¹ with the easy axes of both AF twins in the plane of the sample at 90° to each other.⁴ The hysteresis loop of an Fe(12 nm)/MnF₂(65 nm) bilayer field cooled in 1 kOe and measured at $T = 10 \text{ K}$ is shown in Fig. 1(a). The angular dependence of the EA energy in the Fe/MnF₂ bilayers, $E_{EA}(\alpha_F)$, was measured by a technique utilizing the anisotropic magnetoresistance (AMR) (Refs. 12 and 13); details of the measurements are given in Ref. 7. Figure 1(b) shows $E_{EA}(\alpha_F)$ of Fe/MnF₂ obtained by this technique at $T = 10 \text{ K}$. This complex $E_{EA}(\alpha_F)$ may be phenomenologically described as a combination of unidirectional, uniaxial, threefold and fourfold components.⁷

In order to calculate $E_{EA}(\alpha_F)$ in Fe/MnF₂, we have performed numerical simulations of the EA in this system. Figure 2(a) shows the spin structure of MnF₂ and the AF exchange integrals J_1 , J_{AF} , and J_3 . Since both \mathbf{M}_F and the AF easy axes are in the plane of the sample, the AF spins are also in the sample plane.¹⁴ Thus, the direction of an AF spin may be described by a single angle, α_i^{SL} , where $SL = (A, B)$ denotes the AF sublattice and $i = (1..N)$ enumerates the AF (110) planes starting from the AF/*F* interface [Fig.

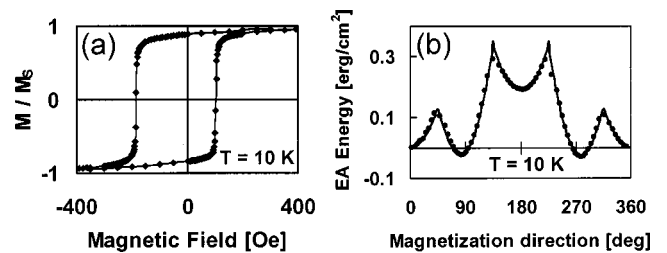


FIG. 1. (a) Hysteresis loop of Fe/MnF₂ bilayer at $T = 10 \text{ K}$; the line is a guide to the eye. (b) Angular dependence of the exchange anisotropy energy per area of Fe/MnF₂ bilayer at $T = 10 \text{ K}$. Circles are experimental data obtained by the AMR technique; the line is a fit to the experimental data using Eq. (2) and a phenomenological uniaxial anisotropy term $K_2 \cos(2\alpha_F)$.

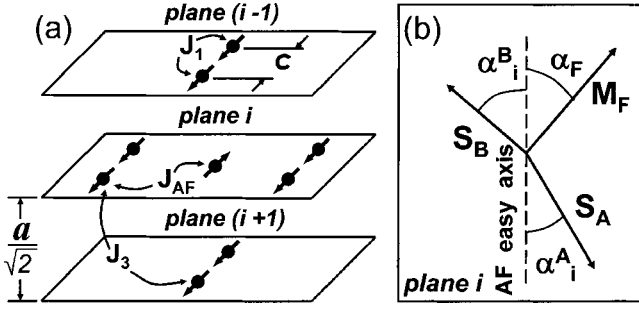


FIG. 2. (a) Spin structure, lattice constants (a , c), and exchange integrals (J_1, J_{AF}, J_3) of MnF_2 . The Mn^{2+} ion in the center is exchange coupled via J_{AF} to four Mn^{2+} ions in the same (110) plane and to two Mn^{2+} ions in each of the two neighboring (110) planes. (b) Definition of the AF spin directions (angles α_i^A and α_i^B) with respect to the AF easy axis in the i th AF (110) plane of MnF_2 . The angle α_F defines the direction of the F magnetization. This illustration is consistent with an antiferromagnetic coupling between the F and the two AF sublattices [11].

2(b)]¹⁵ In order to model the uncompensated interfacial AF spins¹⁶ and unidirectional EA,¹⁷ the spin of one of the AF sublattices in the interfacial ($i=1$) AF (110) plane is assumed to be $S(1+\delta)$ while the spin of the other sublattice is $S(1-\delta)$.¹⁸ The uncompensated spins may be induced by the AF/F interfacial roughness.¹⁹ Only the exchange integral $J_{AF} = -0.152$ meV is important in determining $E_{EA}(\alpha_F)$ because the angle between the spins coupled via J_1 remains 180° , and J_3 is small ($J_3 = -0.004$ meV).²⁰ Therefore, the EA energy per area may be written as

$$E_{EA} = \frac{1}{A} \left[8J_{AF}S^2 \sum_{i=1}^N \cos(\alpha_i^A - \alpha_i^B) + 4J_{AF}S^2 \sum_{i=1}^{N-1} [\cos(\alpha_i^A - \alpha_{i+1}^B) + \cos(\alpha_i^B - \alpha_{i+1}^A)] + \kappa_{AF} \sum_{i=1}^N [\sin^2(\alpha_i^A) + \sin^2(\alpha_i^B)] + 2J_{in}S(1+\delta)\cos(\alpha_1^A - \alpha_F) - 2J_{in}S(1-\delta)\cos(\alpha_1^B - \alpha_F) \right], \quad (1)$$

where S is the AF spin, N is the number of the AF (110) planes in the AF grain ($N=16$ was used in the calculations since the EA energy was found to be essentially independent of N for $N>16$), $A = \sqrt{2} \cdot a \cdot c$ is the surface area per two spins in an AF (110) plane, $\kappa_{AF} = K_{AF}a^2c/2$, and $2J_{in}S(1 \pm \delta)\cos(\alpha_i^{SL} - \alpha_F)$ is the coupling energy between an interfacial AF spin and the F layer with $J_{in} = 4J_{AF}$.²¹ The first term in Eq. (1) is the coupling energy between AF spins in the same (110) plane, the second term describes coupling between AF spins in neighboring (110) planes, the third term is the AF magnetocrystalline anisotropy energy and the last two terms describe the AF/F interfacial coupling.²² The fraction of uncompensated interfacial spins was determined from the AF grain size, L , using the random field model $\delta \approx 1/2\sqrt{n_S}$,¹⁹ where $n_S = \sqrt{2} \cdot L^2/a \cdot c$ is the number of AF spins at the AF/F interface of the AF grain. Scherrer analysis

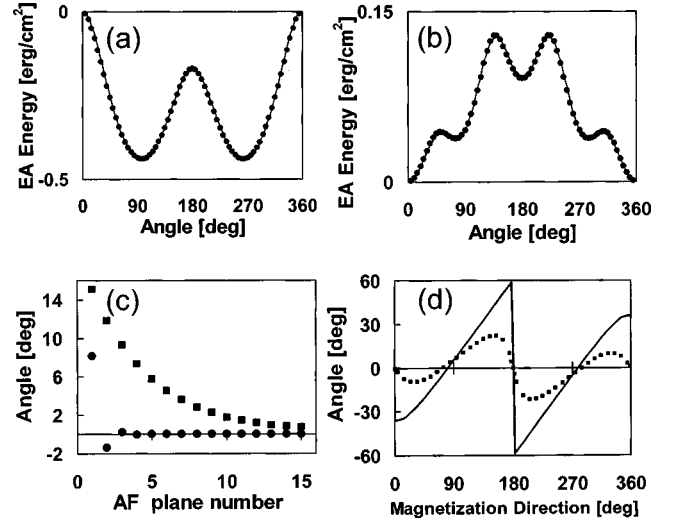


FIG. 3. Angular dependence of the EA energy for a single MnF_2 grain (a) and a twinned MnF_2 layer (b) coupled to an Fe layer calculated numerically using Eq. (1) (circles) and analytically using Eq. (3) (line). (c) Depth profiles of the spin canting angle α_i^{SC} (circles) and domain wall angle α_i^{DW} (squares) in the MnF_2 grain for \mathbf{M}_F at 45° to the AF easy axis. (d) The AF partial domain wall angle α_i^{DW} calculated as a function of the F magnetization direction, α_F , using Eq. (2) for $\delta=0.044$ and two values of J_{in} : $J_{in} = 4J_{AF}$ (squares) and $J_{in} = 6.7J_{AF}$ (solid line).

applied to the full width at half maximum of the in-plane X-ray diffraction at grazing incidence gives $L \approx 10$ nm, which results in $\delta \approx 0.02$.^{23,24}

The energy given by Eq. (1) was minimized with respect to α_i^A and α_i^B ($i=1, \dots, N$) for each value of α_F , and the global energy minimum of the system was found.¹⁵ These calculations give $E_{EA}(\alpha_F)$ for a single AF grain shown in Fig. 3(a). Assuming equal twin populations, the EA energy for a twinned AF layer given by $E_{EA}^{TW}(\alpha_F) = [E_{EA}(\alpha_F + \pi/4) + E_{EA}(\alpha_F - \pi/4)]/2$ is shown in Fig. 3(b). Comparison of $E_{EA}^{TW}(\alpha_F)$ to the data in Fig. 1(b) shows that the model gives a qualitatively correct result for the angular dependence of the EA energy.

Equation (1) includes all the relevant energies for the AF/F exchange coupling, however, an analytical model can be constructed by recasting Eq. (1) in another form which consists of three terms: the AF spin-canting energy,^{16,25,26} the AF domain wall energy,¹⁴ and the direct AF/F exchange coupling energy. For the analytical model, we define two angles, $\alpha_i^{SC} = (\alpha_i^A - \alpha_i^B)/2$ and $\alpha_i^{DW} = (\alpha_i^A + \alpha_i^B)/2$, where α_i^{SC} gives the degree of spin canting between the two sublattices while α_i^{DW} characterizes the uniform rotation of both AF sublattices in the i th AF plane [Fig. 2(b)]. The depth profiles of α_i^{SC} and α_i^{DW} calculated from Eq. (1) for \mathbf{M}_F at 45° to the AF easy axis are shown in Fig. 3(c). As can be seen, the value of α_i^{SC} rapidly decays and it is reasonable to consider the spin canting to occur in only the first two interfacial layers.²⁶ In contrast, the decay of α_i^{DW} is much slower (this is expected since the AF anisotropy energy is much smaller than the AF exchange energy). The angles α_i^{DW} describe a domain wall in the AF layer with its rotation in the

plane of the sample. The energy stored in the AF is given by the sum of the spin canting and the domain wall energies

$$E_{AF} = -2 \frac{J_{SC} S^2}{A} \cos(2\alpha_1^{SC}) - \frac{\sigma}{2} \cos(\alpha_1^{DW}),$$

where σ is the 180° AF domain wall energy ($\sigma = 4\sqrt{A_{EX}K_{AF}}$, with $A_{EX} = 2|J_{AF}|S^2/c$), and J_{SC} is the spin canting energy. Therefore, the EA energy per area is

$$E_{EA} = -\frac{1}{A} \{ 2J_{SC} S^2 \cos(2\alpha_1^{SC}) - 2J_{in} S [(1+\delta)\cos(\alpha_1^A - \alpha_F) - (1-\delta)\cos(\alpha_1^B - \alpha_F)] \} - \frac{\sigma}{2} \cos(\alpha_1^{DW}). \quad (2)$$

Assuming that only the spin-canting angle in the first interfacial AF plane, α_1^{SC} , is nonzero, one can calculate the spin-canting energy per area. This energy consists of three terms: the exchange energy between AF spins in the interfacial AF plane, $(16|J_{AF}|S^2/A)(\alpha_1^{SC})^2$; the exchange energy between the spins in the interfacial plane and the second ($i=2$) plane, $(4|J_{AF}|S^2/A)(\alpha_1^{SC})^2$; and the magnetocrystalline anisotropy energy $(2\kappa_{AF}/A)(\alpha_1^{SC})^2$. Adding these terms, we obtain $J_{SC} \approx 5|J_{AF}| + (\kappa_{AF}/2S^2)$. Retaining nonzero values for both α_1^{SC} and α_2^{SC} and minimizing the coupling energy with respect to α_2^{SC} , we obtain $J_{SC} \approx \frac{29}{6}|J_{AF}| + (37\kappa_{AF}/72S^2)$, where the terms of the order $\kappa_{AF}^2/J_{AF}S^2$ were neglected.

For small values of α_1^{SC} and α_1^{DW} , each term in Eq. (2) is expanded in a Taylor series with respect to α_1^{SC} and α_1^{DW} , and all terms of order higher than quadratic are neglected with the exception of the largest cubic term $(2J_{in}S/A)\alpha_1^{SC}(\alpha_1^{DW})^2 \sin(\alpha_F)$. Retaining of this term improves the model for larger values of α_1^{SC} and α_1^{DW} ; this term may be approximated by a quadratic term

$$\frac{\sigma}{4} \left(\frac{1}{\eta} - 1 \right) (\alpha_1^{DW})^2,$$

where

$$\eta^{-1} = 1 + \frac{\beta \sin^2(\alpha_F)}{1 - \gamma(1+\lambda)\cos(\alpha_F) - \beta \cos^2(\alpha_F)},$$

$\beta = 4J_{in}^2/J_{SC}A\sigma$, $\gamma = 8\delta \cdot S \cdot J_{in}/A\sigma$, and $\lambda = A\sigma/16J_{SC}S^2$.²⁷ Minimizing the expanded and simplified Eq. (2) with respect to α_1^{SC} and α_1^{DW} , we obtain an analytical expression for the EA energy,

$$E_{EA}(\alpha_F) = \frac{1}{A} \left[4\delta \cdot S \cdot J_{in} \cos(\alpha_F) - \frac{J_{in}^2}{J_{SC}} \left\{ \frac{1 + \gamma\eta \cos(\alpha_F)}{1 - \gamma(\eta + \lambda)\cos(\alpha_F) - \beta\eta \cos^2(\alpha_F)} \right\} \times \sin^2(\alpha_F) \right], \quad (3)$$

where small terms proportional to δ^2 were neglected. The solid lines in Figs. 3(a) and 3(b) are given by Eq. (3) with the

same parameters as those used in the numerical calculation. It is clear that the analytical expression given by Eq. (3) is in an excellent agreement with the numerical results. If J_{in} and δ are large so that the condition of small α_1^{SC} and α_1^{DW} is not satisfied, Eq. (2) must be numerically minimized with respect to α_1^{SC} and α_1^{DW} in order to obtain $E_{EA}(\alpha_F)$.

The key parameter determining the magnitude of the EA terms of a higher than uniaxial symmetry is σ . Indeed, if σ is large ($\sigma \gg 4J_{in}^2/J_{SC}A$), the expression in curly brackets in Eq. (3) tends to unity and $E_{EA}(\alpha_F)$ is described by a combination of unidirectional and uniaxial terms. For the twinned AF layer, the uniaxial terms cancel and one is left with a purely unidirectional EA. If, however, σ is small, the higher symmetry EA terms appear in Eq. (3). Expanding Eq. (3) in a Fourier series [$E_{EA}(\alpha_F) = -\sum_n K_n \cos(n\alpha_F)$], we find that for $J_{in} \ll \frac{1}{2}\sqrt{J_{SC}A\sigma}$, $K_3 \sim \delta \cdot S \cdot J_{in}^3/J_{SC}A\sigma$, and $K_4 \sim J_{in}^4/J_{SC}A\sigma$.²⁸ These expressions clarify the role of the partial AF domain wall ($\alpha_1^{DW} \ll \pi$) parallel to the AF/F interface in determining the EA. Previously it was shown that a 180° AF domain wall results in the unidirectional EA proportional to σ .²⁹ It is clear from Eq. (3) that for a partial AF domain wall the unidirectional EA is proportional to $J_{in} \cdot \delta$, while σ determines the magnitude of the higher symmetry EA terms. These terms determine such properties of the bilayer as the enhanced coercivity (K_4) (Ref. 9) and the asymmetric magnetization reversal (K_3).⁷ They also contribute to the complex angular dependence of the hysteresis loop shift and coercivity.^{30,31} Since $K_3/K_4 \sim J_{SC} \cdot \delta \cdot S/J_{in}$, K_3 is expected to dominate over K_4 if the AF/F coupling J_{in} is weak and δ is large. For roughness-induced uncompensated AF spins,¹⁹ the odd symmetry EA terms are expected to be more sensitive to the AF/F interfacial roughness than the even symmetry terms.

The origin of the unusual threefold EA term may be explained by considering the expression of the EA due to the uncompensated AF spins: $(4J_{in} \cdot \delta \cdot S/A)\cos(\alpha_F - \alpha_1^A)$. For large AF magnetocrystalline anisotropy, $\alpha_1^A \approx 0$ for any value of α_F and the EA due to the uncompensated AF spins is purely unidirectional: $(4J_{in} \cdot \delta \cdot S/A)\cos(\alpha_F)$. For a smaller AF anisotropy, a partial AF domain wall is formed, and α_1^A becomes a function of α_F . The resulting EA: $(4J_{in} \cdot \delta \cdot S/A)\cos[\alpha_F - \alpha_1^A(\alpha_F)]$ is a complex function of α_F with higher symmetry odd terms present.^{14,32}

Since $K_1 \sim J_{in} \cdot \delta$ and $K_4 \sim J_{in}^4/J_{SC}A\sigma$, the data in Fig. 1(b) enable us to *separately* determine δ and J_{in} while the hysteresis loop shift only gives their product, $J_{in} \cdot \delta$. The solid line in Fig. 1(b) is the fit of the expression $E(\alpha_F) = [E_{EA}(\alpha_F + \pi/4) + E_{EA}(\alpha_F - \pi/4)]/2 - K_2 \cos(2\alpha_F)$, with $E_{EA}(\alpha_F)$ given by Eq. (2) to the experimental data, with J_{in} , δ , and K_2 as fitting parameters. Inclusion of a phenomenological uniaxial anisotropy term $K_2 \cos(2\alpha_F)$ with $K_2 = -0.056 \text{ erg/cm}^2$ improves the fit to the experimental data. As predicted by a recent theoretical study,³³ the uniaxial anisotropy term K_2 may originate from an inhomogeneous exchange coupling over the AF/F interface. The values of $\delta = 0.044$ and $J_{in} = 6.7J_{AF}$ obtained from the fit are large enough so that the conditions $\alpha_1^{SC} \ll 1$ and $\alpha_1^{DW} \ll 1$ are not satisfied, and Eq. (2) is used to fit the data instead of Eq. (3).

This fitting procedure with three fitting parameters (δ , J_{in} , and K_2) gives a better fit to the data than a phenomenological expression $E(\alpha_F) = -K_1 \cos(\alpha_F) - K_2 \cos(2\alpha_F) - K_3 \cos(3\alpha_F) - K_4 \cos(4\alpha_F)$ with four fitting parameters (K_1 , K_2 , K_3 , and K_4) as used in Ref. 7. This is because the latter expression does not reproduce the sharp EA energy peaks along the AF easy axes of the MnF_2 twins. The origin of these sharp peaks is the abrupt change of sign of α_1^{DW} as the AF domain wall changes its chirality when \mathbf{M}_F rotates through the AF easy axis.¹⁵ This is clarified in Fig. 3(d), that shows the AF domain wall angle α_1^{DW} calculated from Eq. (2) as a function of α_F for $\delta=0.044$ and two values of J_{in} : $J_{\text{in}}=4J_{\text{AF}}$ (squares) and $J_{\text{in}}=6.7J_{\text{AF}}$ (solid line). It is clear from this figure that for $J_{\text{in}}=4J_{\text{AF}}$, α_1^{DW} continuously goes through zero as \mathbf{M}_F passes the AF easy axis. However, for

$J_{\text{in}}=6.7J_{\text{AF}}$, α_1^{DW} abruptly changes sign via an out-of-plane rotation¹⁵ as \mathbf{M}_F passes the AF easy axis, resulting in sharp peaks of the EA energy.

An analytical model describing exchange anisotropy in AF/ F bilayers with an epitaxial AF layer was developed. The model explains the origin of the high symmetry exchange anisotropy terms in AF/ F bilayers as arising from a partial AF domain wall parallel to the AF/ F interface. Application of the model to the experimental data analysis of exchange anisotropy in Fe/ MnF_2 bilayers allows one to separately determine the fraction of uncompensated interfacial spins in the AF layer and the interfacial exchange coupling energy between the AF and F spins.

This work was supported by the MRSEC, the U.S. DOE, the NSF, and the Catalan DGR (2001SGR00189).

-
- ¹W. H. Meiklejohn and C. P. Bean, Phys. Rev. **102**, 1413 (1956).
²J. Nogués and Ivan K. Schuller, J. Magn. Magn. Mater. **192**, 203 (1999).
³M. R. Fitzsimmons, P. Yashar, C. Leighton, Ivan K. Schuller, J. Nogués, C. F. Majkrzak, and J. A. Dura, Phys. Rev. Lett. **84**, 3986 (2000).
⁴C. Leighton, M. R. Fitzsimmons, P. Yashar, A. Hoffmann, J. Nogués, J. Dura, C. F. Majkrzak, and Ivan K. Schuller, Phys. Rev. Lett. **86**, 4394 (2001).
⁵V. I. Nikitenko, V. S. Gornakov, A. J. Shapiro, R. D. Shull, Kai Liu, S. M. Zhou, and C. L. Chien, Phys. Rev. Lett. **84**, 765 (2000).
⁶R. L. Stamps, J. Phys. D **33**, R247 (2000); Miguel Kiwi, J. Magn. Magn. Mater. **234**, 584 (2001).
⁷I. N. Krivorotov, C. Leighton, J. Nogués, Ivan K. Schuller, and E. Dan Dahlberg, Phys. Rev. B **65**, 100402 (2002).
⁸Michael J. Pechan, Douglas Bennett, Nienchtze Teng, C. Leighton, J. Nogués, and Ivan K. Schuller, Phys. Rev. B **65**, 064410 (2002).
⁹Y. J. Tang, B. Roos, T. Mewes, S. O. Demokritov, B. Hillebrands, and Y. J. Wang, Appl. Phys. Lett. **75**, 707 (1999).
¹⁰U. Gäfvert, L. Lundgren, P. Nordland, B. Westerstrandh, and O. Beckman, Solid State Commun. **23**, 9 (1977).
¹¹C. Leighton, J. Nogués, H. Suhl, and Ivan K. Schuller, Phys. Rev. B **60**, 12 837 (1999).
¹²E. D. Dahlberg, K. T. Riggs, and G. A. Prinz, J. Appl. Phys. **63**, 4270 (1988).
¹³B. H. Miller and E. D. Dahlberg, Appl. Phys. Lett. **69**, 3932 (1996).
¹⁴M. D. Stiles and R. D. McMichael, Phys. Rev. B **59**, 3722 (1999).
¹⁵We have done numerical calculations for three-dimensional AF spins and found that all the AF spins lie in the sample plane except in the case of \mathbf{M}_F being collinear with the AF easy axis. In this case the AF spins may rotate out of plane, allowing the system to be in the global energy minimum (without spin switching allowed deep inside of the AF layer) and to avoid metastable states (Ref. 25). As shown in Ref. 16, these metastable states are unphysical and lead to a shifted hysteresis loop even in the absence of the uncompensated AF spins. Calculations of EA for the two-dimensional spins described by Eq. (1) give correct results if a global energy minimum constraint is added.
¹⁶T. C. Schulthess and W. H. Butler, Phys. Rev. Lett. **81**, 4516 (1998).
¹⁷The unidirectional EA may also originate from Dzyaloshinskii-Moriya interaction at the AF/ F interface [Thomas Schulthess (private communication)].
¹⁸The model assumes that EA is determined by the spins in the AF grains while the spins in the AF grain boundaries have no significant effect on the EA.
¹⁹A. P. Malozemoff, Phys. Rev. B **35**, 3679 (1987).
²⁰O. Nikotin, P. A. Lindgard, and O. W. Dietrich, J. Phys. C **2**, 1168 (1969).
²¹The exchange coupling energy between an interfacial AF spin and the F layer can be expressed as $J_{\text{in}} = \sum_j^m J_{\text{AF}/F}^j S_F^j$, where m is the number of F spins (S_F^j) exchange coupled to the interfacial AF spin with exchange integrals $J_{\text{AF}/F}^j$. This quantity can only be calculated if a detailed structure of the AF/ F interface is known. For the illustration purpose we use $J_{\text{in}}=4J_{\text{AF}}$ in our calculations.
²²A partial domain wall in the F layer is important for determining the magnetic properties of the system if the applied field magnitude is comparable to the exchange bias and coercive fields (Ref. 26). However, for applied fields much larger than the exchange and coercive fields such as those used in our AMR measurements, the F domain wall angle becomes small and it may be neglected.
²³An AF grain in contact with F may break up onto domains of size $\ell = \pi \sqrt{A_{\text{EX}}/K_{\text{AF}}}$ (Ref. 19) (for MnF_2 , $\ell = 5$ nm). Since the AF domain wall width is also ℓ and the MnF_2 grain size is 10 nm, the MnF_2 grains are in a single domain state and Eq. (1) applies, otherwise a three-dimensional problem for the AF spins must be solved numerically (Ref. 24).
²⁴P. Miltényi, M. Gierlings, J. Keller, B. Beschoten, G. Güntherodt, U. Nowak, and K. D. Usadel, Phys. Rev. Lett. **84**, 4224 (2000).
²⁵N. C. Koon, Phys. Rev. Lett. **78**, 4865 (1997).
²⁶M. Kiwi, J. Mejía-López, R. D. Portugal, and R. Ramírez, Appl. Phys. Lett. **75**, 3995 (1999).
²⁷The leading cubic term $(2J_{\text{in}}S/A)\alpha_1^{\text{SC}}(\alpha_1^{\text{DW}})^2 \sin(\alpha_F)$ can be ap-

proximated by a quadratic term if one uses an approximate solution

$$\alpha_1^{\text{SC}} \approx - \frac{J_{\text{in}} \sin(\alpha_F)}{2S \cdot J_{\text{SC}} [1 - \gamma(1 + \lambda) \cos(\alpha_F) - \beta \cos^2(\alpha_F)]}$$

obtained from the Taylor expansion of Eq. (2) neglecting all cubic and higher order terms.

²⁸An expression for the angular dependence of the EA energy was also derived in Ref. 14 in the limit of zero perpendicular coupling and thus it neglects the even symmetry terms.

- ²⁹D. Mauri, H. C. Siegmann, P. S. Bagus, and E. Kay, *J. Appl. Phys.* **62**, 3047 (1987).
³⁰T. Ambrose, R. L. Sommer, and C. L. Chien, *Phys. Rev. B* **56**, 83 (1997).
³¹Haiwen Xi, Mark H. Kryder, and Robert M. White, *Appl. Phys. Lett.* **74**, 2687 (1999).
³²Joo-Von Kim, R. L. Stamps, B. V. McGrath, and R. E. Camley, *Phys. Rev. B* **61**, 8888 (2000).
³³B. Heinrich, T. Monchesky, R. Urban, *J. Magn. Mater.* **236**, 339 (2001).